Regulation of RhoA GTP Hydrolysis by the GTPase-Activating Proteins p190, p50RhoGAP, Bcr, and 3BP-1[†]

Baolin Zhang and Yi Zheng*

Department of Biochemistry, University of Tennessee, Memphis, Tennessee 38163

Received July 29, 1997; Revised Manuscript Received February 16, 1998

ABSTRACT: The small GTP-binding protein RhoA becomes inactivated by hydrolyzing bound GTP to GDP through its intrinsic GTPase activity which is further stimulated by a family of Rho GTPase-activating proteins (GAPs). Here we have compared the kinetics of interaction between recombinant RhoA and the RhoGAP domains of p190, p50RhoGAP, Bcr, and 3BP-1. The intrinsic rate of GTP hydrolysis by RhoA is relatively slow when compared to other Rho-family GTPases such as Cdc42 or Rac1 with a rate constant of 0.022 min^{-1}, which can be further stimulated at least 4000-fold by p190 or p50RhoGAP. The RhoGAP domains of Bcr and 3BP-1, which were thought to be inactive toward RhoA, are also found capable of stimulating the GTPase activity of RhoA in a dose-dependent manner. The supreme catalytic activities of p190 and p50RhoGAP toward RhoA reside mostly in their lower K_m values (1.79 and 2.83 μM, respectively) which correlate well with their binding affinity for GMP-PNP-bound RhoA (2.18 and 2.47 μM, respectively), in contrast with Bcr and 3BP-1 which interact with the activated RhoA with much higher K_m (89 μM). However, the mechanisms of catalysis by p190 and p50RhoGAP are distinct in at least three aspects: (1) p50RhoGAP displays an effect of product inhibition by binding to the GDP-bound form of RhoA with a K_d of 6 μM in comparison with the K_d for p190 of 33 μM; (2) the K_m of p190 increases drastically upon the increase of salt and Mg^{2+} concentrations, conditions under which only modest changes of K_m for p50RhoGAP are observed; and (3) p50RhoGAP remains partially active toward the effector domain mutants of RhoA, Y34K, and T37A, whereas p190 is completely inactive toward Y34K and T37A. These results suggest that there exists a unique mechanism of functional interaction between RhoA and individual RhoGAP which involves distinct structural determinants of the small G-protein to cause the apparent differences in kinetic properties.

Members of the mammalian Rho GTPase family, including RhoA, Rac1, and Cdc42, appear to play key roles in controlling cell actin−cytoskeleton organization, gene transcription, and cell proliferation (*1*−*3*). RhoA, in particular, has been shown to regulate the actin-dependent processes such as platelet aggregation (*4*), lymphocyte adhesion (*5*), cell motility (*6*, *7*), and cytokinesis (*8*). Microinjection of activated RhoA into fibroblast cells causes rapid formation of actin stress fibers and focal adhesions while inactivation of RhoA leads to reversion of these effects (*9*), indicating that RhoA mediates the signal flow linking extracellular stimuli to reorganization of the actin cytoskeleton. Evidence implicating RhoA as a regulator of cell growth control and gene activation includes that a number of Rho-specific guanine exchange factors are potent oncogene products (*10*), that RhoA apparently is required for Ras-induced transformation (*11*, *12*) and is capable of activating serum response factors (*13*), and that microinjection of the active form of RhoA into fibroblasts stimulates DNA synthesis (*14*).

It is becoming clear that the biochemical activity of RhoA is highly regulated in these biological processes. Like other small GTP-binding proteins, RhoA cycles between the GTP-bound active and the GDP-bound inactive states and becomes inactivated due to its intrinsic GTPase activity which is further stimulated by the GTPase-activating proteins (GAPs)[1] (*15*). The GAPs specific for Rho-family GTPases include over 10 mammalian proteins, many of which are large multifunctional signal transducers with a potential to serve as either negative regulators or downstream targets of Rho GTPases through their ability to interact with specific Rho proteins and with additional cytosolic factors. They all share a homologous RhoGAP domain spanning ∼200 amino acids responsible for the GAP activity (*16*, *17*). Recently available crystallography data of GAP domains of the p85 regulatory subunit of PI3-kinase (*18*) and p50RhoGAP (*19*) indicate that this domain adopts a highly conserved three-dimensional folding and suggest that a similar mechanism may be at work for RhoGAPs to utilize a few charged residues exposed at a putative G-protein-binding α-helical pocket to catalyze the GTPase activity of Rho proteins.

To examine the mechanism of regulation of RhoA by RhoGAPs, we set out in the present study to derive kinetic parameters involved in the interaction between RhoA and

[†]This work was supported in part by American Cancer Society Grant RPG-97-146-01 and National Institutes of Health Grant GM53943 (to Y.Z.).

* To whom correspondence should be addressed. Telephone: (901) 448-5138. Fax: (901) 448-7360. E-mail: yzheng@utmem1.utmem.edu.

[1] Abbreviations: Bcr, breakpoint cluster region gene product; BSA, bovine serum albumin; GAP, GTPase-activating protein; GMP-PNP, guanylyl imidodiphosphate; GST, glutathione *S*-transferase; MESG, 2-amino-6-mercapto-7-methylpurine ribonucleoside.

S0006-2960(97)01844-8 CCC: $15.00
Published on Web 03/24/1998

GAP domains of four mammalian GAPs: the RasGAP-binding phosphoprotein p190, which is a Rho-specific GAP (*20*, *21*); the p50RhoGAP (also known as Cdc42GAP), which contains a rather broad spectrum of GAP activity for Rho-family GTPases but seems more active toward Cdc42 (*22*, *23*); the breakpoint cluster region gene product (Bcr), which was shown to be a Rac-specific downregulator (*21*, *24*); and the Abl-SH3 domain-binding protein 3BP-1, which represents a GAP activity primarily toward Rac and Cdc42 (*25*). The aim is to directly compare the kinetics of the GAP reactions of RhoA to provide clues to where some of the apparent specificities of the interaction may arise and to reveal unique mechanisms involved. Based upon a spectroscopic method developed by Webb (*26*), we were able to monitor the continuous release of γ-P_i from RhoA-GTP using a P_i-specific phosphorylase and to follow the proceedings of GTP hydrolysis under single-turnover conditions. We found that while the RhoGAP domains of p190 and p50RhoGAP contain comparable catalytic activity toward RhoA, Bcr, and 3BP-1, which were thought to be inactive toward RhoA (*24*, *25*), are also capable of stimulating the GTPase activity of RhoA in a dose-dependent manner. The supreme catalytic activities of p190 and p50RhoGAP toward RhoA reside mostly in their lower K_m values which correlate well with their binding affinities for GMP-PNP-bound RhoA. Moreover, our results suggest that the distinctive mechanisms of interaction between p190 and RhoA and between p50RhoGAP and RhoA displayed by the diverse properties of product (Rho-GDP) inhibition and sensitivity to salt may be attributed to different structural requirements of RhoA GTPase involved in the respective interactions. We conclude that there exists a unique mechanism for each specific interaction between RhoA and a RhoGAP.

EXPERIMENTAL PROCEDURES

Materials. Guanylyl imidodiphosphate (GMP-PNP) was from Boehringer-Manheim. [γ-^{32}P]GTP (6000 Ci/mmol) was obtained from NEN-DuPont. GDP, GTP, bacterial purine nucleoside phosphorylase, and the ingredients to synthesize the phosphorylase substrate, 2-amino-6-mercapto-7-methylpurine ribonucleoside (MESG), were purchased from Sigma. MESG was synthesized following the published protocol (*26*) and was stored in a lyophilized form at −20 °C. The absorbance response of MESG at 360 nm for measuring a range of P_i concentrations from 1 to 80 μM in a phosphate buffer (pH 7.6) was calibrated by using the coupling reaction of purine nucleoside phosphorylase (*26*).

Expression and Purification of Recombinant Proteins. Human RhoA protein was expressed in *E. coli* as $(His)_6$-tagged fusion by using the pET expression system (Novagen). Briefly, the cDNA encoding RhoA was cloned into pET28a vector at the in-frame *Bam*HI−*Eco*RI sites, and the resulting construct was transformed into competent BL21 cells. The induction and purification of $(His)_6$-tagged RhoA by isopropyl β-thiogalactopyranoside and Ni^{2+}-charged agarose beads were carried out following the instructions provided by Novagen. Mutant cDNAs of RhoA were generated by polymerase chain reactions as described (*27*), and were cloned into the pGEX-KG vector to be expressed as glutathione *S*-transferase (GST) fusions. The GAP domains of p190, p50RhoGAP, Bcr, and 3BP-1, which contain amino acid residues 1249−1513, 205−439, 1010−1271, and 185−410 of the native proteins, respectively, were also expressed in *E. coli* using the pGEX system (*28*). Production and purification of the GST fusions from *E. coli* were carried out as described by glutathione affinity chromotography (*17*). All proteins prepared for measurements were subjected to sodium dodecyl sulfate−polyacrylamide gel electrophoresis and coomassie-blue staining analysis, and the contents of each were judged at least 90% pure. Since it has been found that the GST moiety attached to the GAP domains does not affect on the catalytic efficiencies of the GAPs (*28*), all kinetic measurements performed in this study utilized the intact GST−GAP fusions. If necessary, the $(His)_6$ moiety of the small G-protein fusions was cleaved by thrombin digestion followed by incubation with *p*-aminobenzamidine immobilized on agarose beads (Sigma) to remove the thrombin (*29*). Concentrations of the recombinant GST−GAPs were determined using the BCA protein assay reagents from Pierce with bovine serum albumin (BSA) as a standard, and the effective concentration of RhoA was measured using the MESG/phosphorylase system under single-turnover conditions as described below.

GTPase Activity Assays. The radioactive filter-binding assay measuring the retention of [γ-^{32}P]GTP-bound RhoA was carried out as described (*17*). Briefly, recombinant RhoA was preloaded with [γ-^{32}P]GTP (10 μCi, 6000Ci/mmol, NEN) in a 100 μL buffer containing 50 mM HEPES, pH 7.6, 0.2 mg/mL BSA, and 0.5 mM EDTA for 10 min at ambient temperature before the addition of $MgCl_2$ to a final concentration of 5 mM. An aliquot of the [γ-^{32}P]GTP-loaded RhoA was mixed with a reaction buffer containing 50 mM HEPES, pH 7.6, 0.2 mg/mL BSA, and 10 mM $MgCl_2$ in the presence or absence of GAP. At different time points, the reaction was terminated by filtering the reaction mixture through nitrocellulose filters followed by washing with 10 mL of ice-cold buffer containing 50 mM HEPES, pH 7.6, and 10 mM $MgCl_2$. The radioactivity retained on the filters was then subjected to quantitation by scintillation counting. In the competition assays to determine the binding affinity of GAP domains to RhoA, GST−GAP domains at the indicated concentrations together with the indicated amount of RhoA preloaded with GMP-PNP or GDP were present in the reaction mixture in addition to the components described above and 20 nM RhoA-[γ-^{32}P]GTP, and the reactions were terminated after a 5 min incubation at 20 °C.

The MESG/phosphorylase system monitoring γ-P_i release from RhoA-GTP was based on the method described by Webb and Hunter (*30*) and has been applied to the measurement of GTPase activity of the Rho-family small GTPase Cdc42 (*28*). Briefly, a 0.8 mL solution containing 50 mM HEPES, pH 7.6, 0.1 mM EDTA, 0.2 mM MESG, 10 units of purine nucleoside phosphorylase, 200 μM GTP, and the indicated amount of recombinant RhoA was mixed in a 4 mm width, 10 mm path length cuvette, and the time courses of the absorbance change at 360 nm were recorded. Single-turnover GTPase reactions were initiated by the addition of $MgCl_2$ to a final concentration of 5 mM. For measurement of GAP-catalyzed reactions, 5−50 μL of stock solution containing the indicated amount of GAP was added together with $MgCl_2$ to the reaction mixtures. Control experiment in which RhoA was left out was carried out to provide a background of absorbance in each independent measurement to be subtracted from the sample signals. The concentration

of P_i in the reaction solution is proportional to the net absorbance change by a factor of extinction coefficient $\epsilon_{360\ nm} = 11\,000\ M^{-1}\ cm^{-1}$ at pH 7.6 (*30*), and was used to determine the concentration of RhoA after one round of single-turnover reaction. Because the phosphorylase coupling reaction is extremely fast with a rate constant of 40 s^{-1} (*26*), the slope of the absorbance in the time course is treated as proportional to the rate of the GTPase activity of RhoA:

$$\text{rate of RhoA-GTP hydrolysis} = 1/\epsilon_{360\ nm} \times \Delta A\ cm^{-1}\ min^{-1}\ M^{-1}$$

Data Analysis. Kinetic data were analyzed by nonlinear regression with the program Enzfitter (Elsevier Biosoft) as described (*28*). The rate constant (K_c) of intrinsic GTP hydrolysis by RhoA was determined by fitting data obtained by the MESG system or by filter-binding assay to a single-exponential function. Since the amount of RhoA present in the GAP reaction is in great excess of GAPs, a modified Michaelis−Menten equation was used to derive kinetic parameters assuming GAP is acting as the enzyme catalyst, RhoA-GTP as the substrate, and RhoA-GDP and P_i as the products:

$$V_0 = \epsilon V_{max}[RhoA]_0/(K_m + [RhoA]_0) + \epsilon K_c[RhoA]_0 \quad (1)$$

where V_0 is the initial rate of hydrolysis, ϵ is the extinction coefficient at 360 nm for the phosphorylase reaction product, $[RhoA]_0$ is the total RhoA concentration, K_c is the rate constant of intrinsic GTPase activity, and the term $\epsilon K_c[RhoA]_0$ is a correction for the rate of intrinsic GTP hydrolysis by RhoA. K_{cat} is derived by $V_{max}/[GAP]_0$ with $[GAP]_0$ representing total GAP concentration.

To determine the affinity of GAPs to RhoA, the competition assay involving RhoA-[γ-^{32}P]GTP, GST−GAP, and competitor C (GMP-PNP- or GDP-bound RhoA) was described by two simultaneous reactions:

$$\text{GAP} + [\gamma\text{-}^{32}\text{P}]\text{GTP-RhoA} \rightleftharpoons [\gamma\text{-}^{32}\text{P}]\text{GTP-RhoA}\cdot\text{GAP} \rightleftharpoons \text{GAP} + \text{RhoA-GDP} + [\gamma\text{-}^{32}\text{P}]P_i$$

and

$$\text{GAP} + \text{C} \rightleftharpoons \text{GAP−C};\ \text{with}\ K_d = [\text{GAP}][\text{C}]/[\text{GAP−C}]$$

and the dissociation constants (K_d) were derived by fitting data to the following derived equation under the conditions that the concentration of RhoA-[γ-^{32}P]GTP (20 nM) is orders of magnitude smaller than the total concentration of competitor $[C]_0$ and reaction K_m value:

$$\text{inhibition of GAP-catalyzed GTP hydrolysis \%} = 1 - K_d/(K_d + [C]_0) \quad (2)$$

RESULTS

Stimulation of the Intrinsic GTPase Activity of RhoA by GAPs. To determine the rate of intrinsic GTP hydrolysis by RhoA, the time courses of GTPase reaction of RhoA under single-turnover conditions were monitored by both the [γ-^{32}P]GTP filter-binding assay and the MESG/phosphorylase assay (Figure 1). In the former assay, the [γ-^{32}P]GTP remaining bound to RhoA was quantitated at discontinuous time points, while the latter assay monitored the absorbance trace at 360 nm wavelength continuously, which reflects γ-P_i release from RhoA-GTP by the phosphorylase coupling reaction with MESG as a substrate. The time courses of RhoA GTPase reaction at 20 °C measured by the two assays showed excellent agreement, and fittings of the data to a single-exponential function yielded an identical intrinsic rate constant (K_c) of 0.022 min^{-1} (Table 1) which is over 3-fold slower than Cdc42 measured under similar conditions (*28*). These results also further ensure that the MESG/phosphorylase assay is a reliable method for the measurement of the GTPase activity of RhoA.

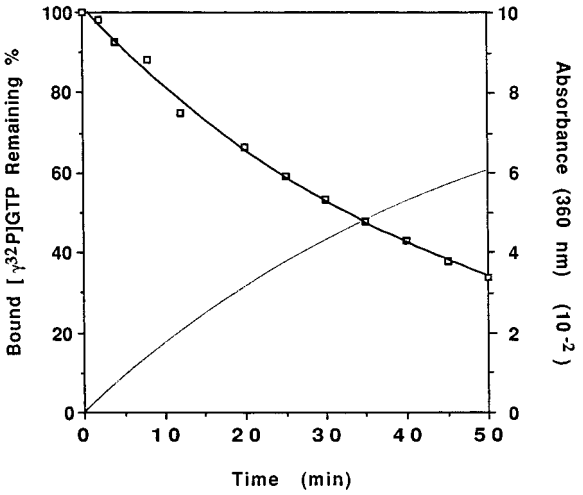

FIGURE 1: Comparison of the time courses for single-turnover GTP hydrolysis by RhoA measured by the MESG system and by radioactive filter binding assay. Recombinant RhoA (7.8 or 0.1 μM) was preloaded with GTP or [γ-^{32}P]GTP at 20 °C and stabilized in 5 mM $MgCl_2$ at time 0. The GTPase reactions were conducted at 20 °C under conditions described under Experimental Procedures, and the absorbance change at 360 nm wavelength or the retention of [γ-^{32}P]GTP bound to RhoA was recorded. Data were best fitted into a single exponential to derive the intrinsic rate constant of RhoA.

Figure 2A shows the absorbance traces for three different reactions with the same amount of RhoA but by addition of different amounts of p190GAP to initiate the reaction. The initial rates of the reactions were linear with p190GAP concentrations up to 80 nM (Figure 2A, insert), which provide the window for determination of p190GAP-catalyzed reaction kinetics. Similarly, the initial rates of p50RhoGAP-stimulated GTPase reaction of RhoA were also found to be linear with p50RhoGAP concentration up to 80 nM (Figure 2B, insert). Interestingly, the kinetic traces of the p50RhoGAP-catalyzed reaction displayed an early plateau phase at higher concentrations of p50RhoGAP (Figure 2B) which was not detected in the case for p190GAP. This observation is consistent with the later finding of the unique property of product inhibition for p50RhoGAP-catalyzed reaction.

As a comparison with p190GAP and p50RhoGAP, we also examined the GAP domains of Bcr and 3BP-1, two of the RhoGAP family members which previously have been shown to be inactive toward RhoA (*24*, *25*, *31*), for their ability to interact with RhoA. To our surprise, both Bcr and 3BP-1 demonstrated dose-dependent activities to stimulate [γ-^{32}P]GTP

Table 1: Kinetic Parameters of RhoA GTPase Regulated by GAPs under Single-Turnover Conditions[a]

GAP	K_c[b] (min^{-1})	V_{max} (μM/min)	K_{cat} (min^{-1})	K_m (μM)	K_{cat}/K_m ($min^{-1}\,\mu M^{-1}$)
–	0.022 ± 0.008	–	–	–	–
p190		3.51 ± 0.06	96.6 ± 1.8	1.79 ± 0.14	54.0 ± 0.9
p50RhoGAP		2.98 ± 0.06	59.6 ± 1.2	2.83 ± 0.16	21.0 ± 0.6
Bcr		4.93 ± 0.43	79.5 ± 7.0	89.4 ± 10.5	0.9 ± 0.1
3BP-1		3.39 ± 1.0	11.8 ± 3.5	89.7 ± 33.9	0.1 ± 0.04

[a] The V_{max} and K_m values were from nonlinear regression analysis using the modified Michaelis−Menten equation (eq 1) as shown in Figure 4, and K_{cat} and K_{cat}/K_m were derived thereon. Data were obtained by the MESG method unless otherwise indicated. GAP reactions were performed under single-turnover conditions as described under Experimental Procedures with GAP domains of 35 nM for p190GAP, 50 nM for p50RhoGAP, 62 nM for Bcr, or 286 nM for 3BP-1 in a buffer containing 50 mM HEPES, pH 7.6, 5 mM $MgCl_2$, 0.2 mM MESG, 10 units/mL purine nucleotide phosphorylase, and 200 μM GTP. The concentrations of GAPs are within the linear range of absorbance change for GAP-stimulated RhoA-GTP hydrolysis. Results are representative of at least two independent measurements. [b] Rate constant for intrinsic GTP hydrolysis by RhoA determined by the MESG/P_i release assay. The value for K_c determined by the filter binding assay was 0.022 ± 0.001 min^{-1}.

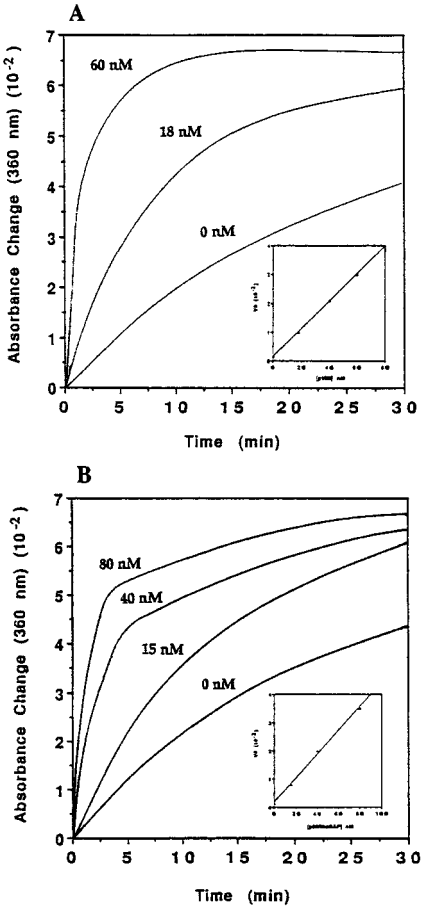

FIGURE 2: Stimulations of the GTPase activity of RhoA by p190GAP and p50RhoGAP measured by the MESG method. (A) Time courses of γ P_i release from RhoA-GTP (5.72 μM) in the presence of different doses of p190GAP. (B) Time courses of GTP hydrolysis by RhoA (5.72 μM) stimulated by different doses of p50RhoGAP. The reactions were initiated by adding the respective GAPs at the indicated concentrations together with 5 mM $MgCl_2$. Inserts: initial rates of P_i release from RhoA-GTP as a function of the GAP concentrations fitted into a linear equation.

hydrolysis by RhoA (Figure 3A,B), albeit they occurred in the presence of much higher concentrations of the respective GAPs (in the micromolar range) than p190GAP or p50RhoGAP. We conclude that these two GAP domains are also capable of interacting with the GTP-bound RhoA and possess weak GAP activity.

Kinetics of Interaction of RhoA-GTP with GAPs. To determine the kinetics of GAP-stimulated hydrolysis by RhoA, the initial rate of P_i release by RhoA-GTP was measured as a function of RhoA concentration at a fixed concentration of GAP, as shown for the case of p190GAP in Figure 4A. Since the amount of RhoA is in large excess of GAPs, the reaction can be treated by Michaelis−Menten kinetics with the adjustment for the intrinsic rate of GTP hydrolysis by RhoA (eq 1 of the Experimental Procedures). Fitting of the data obtained for p190GAP, p50RhoGAP, Bcr, and 3BP-1 yielded a range of K_m and V_{max} values (Figure 4B, Table 1). While both p190GAP and p50RhoGAP gave similar K_m values at 1.79−2.83 μM, Bcr and 3BP-1 shared a K_m value of 89 μM which is over an order of magnitude larger. The K_{cat} values were further derived from V_{max} (Table 1) assuming that all GAPs present were active, although this may lead to an underestimation if a fraction of the GAP was rendered inactive during the preparation procedures. The differences in K_{cat} of various GAPs are less dramatic than in K_m, particularly when considering that Bcr, a rather weak GAP for RhoA, presented a similar K_{cat} value as p190GAP and p50RhoGAP. To rule out the possibility that the amino-terminal $(His)_6$-tag in the small GTPase might influence the intrinsic or GAP-mediated GTPase reaction, additional experiments were carried out with $(His)_6$-tag-cleaved RhoA protein. Essentially identical results were obtained with the tag-cleaved RhoA in both cases of the intrinsic (K_c value at 0.022 ± 0.006 min^{-1}) and p50RhoGAP-catalyzed (K_m value at 3.01 ± 0.41 μM and K_{cat} at 54.0 ± 2.0 min^{-1}) reactions, indicating that the amino portion of the fusion in RhoA does not interfere with the RhoA−GAP interaction. Overall, the catalytic efficiencies (K_{cat}/K_m) of these GAP domains are in the order of p190GAP > p50RhoGAP ≫ Bcr > 3BP-1, and the difference in K_m seems to be a major factor for the varied ability of the GAPs to stimulate GTP hydrolysis of RhoA.

RhoA Binding to GAPs. The affinity of RhoA binding to GAPs at steady state was investigated by measuring the ability of GMP-PNP (a nonhydrolyzable GTP analogue) bound RhoA to inhibit competitively the GAP-stimulated hydrolysis of [γ-^{32}P]GTP-bound RhoA (Figure 5). The concentration range in which RhoA-GMP-PNP inhibits GAP-mediated GTP hydrolysis is an indication of its affinity (K_d) for GAP. By fitting the data to eq 2 described under Experimental Procedures, we have determined that p190GAP bound to RhoA-GMP-PNP with a K_d of 2.18 μM and p50RhoGAP bound with a K_d of 2.47 μM whereas Bcr and 3BP-1 bound with relatively low affinity of 21 and 16 μM, respectively (Table 2). The K_d values of p190 and p50RhoGAP compare well with the K_m values obtained for the GAPs (Tables 1 and 2), suggesting a rapid equilibrium binding of these two GAPs to RhoA-GTP which is not a

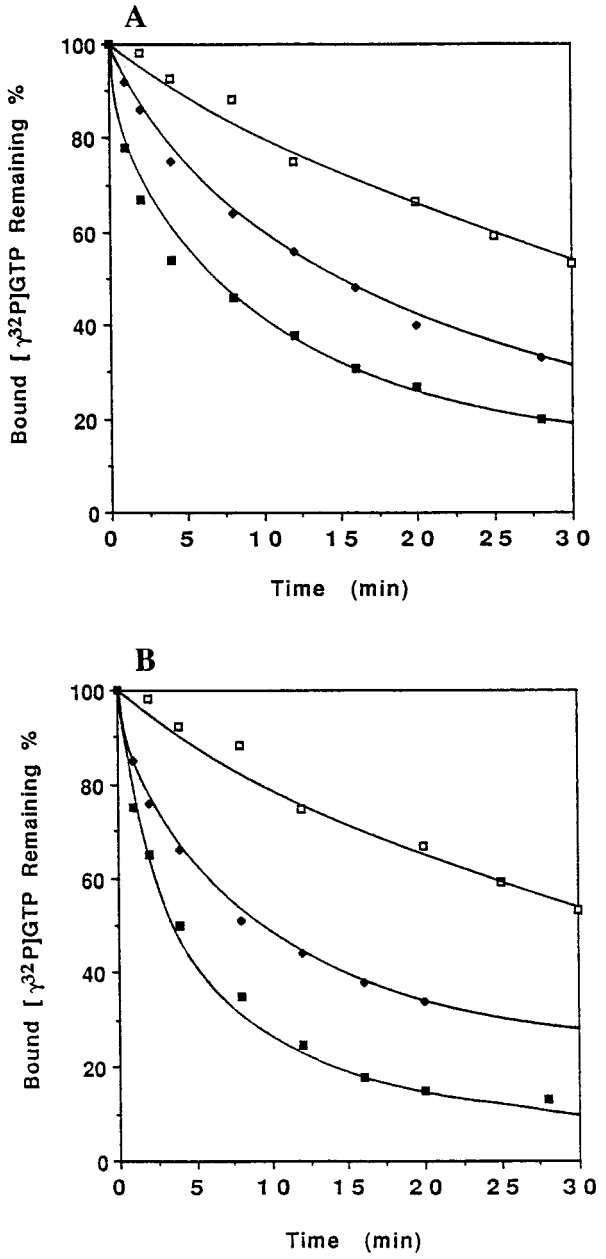

FIGURE 3: Dose-dependent activations of the GTPase activity of RhoA by Bcr and 3BP-1. (A) [γ-^{32}P]GTP-bound RhoA (100 nM) was assayed for the hydrolysis of GTP in the absence (open squares) and presence of 0.44 μM (diamonds) or 2.6 μM (closed squares) Bcr. (B) GTP hydrolysis of 100 nM RhoA was monitored over time in the absence (open squares) or presence of 1.9 μM (diamonds) or 7.8 μM (closed squares) 3BP-1. Reaction conditions were as described under Experimental Procedures for filter binding assays.

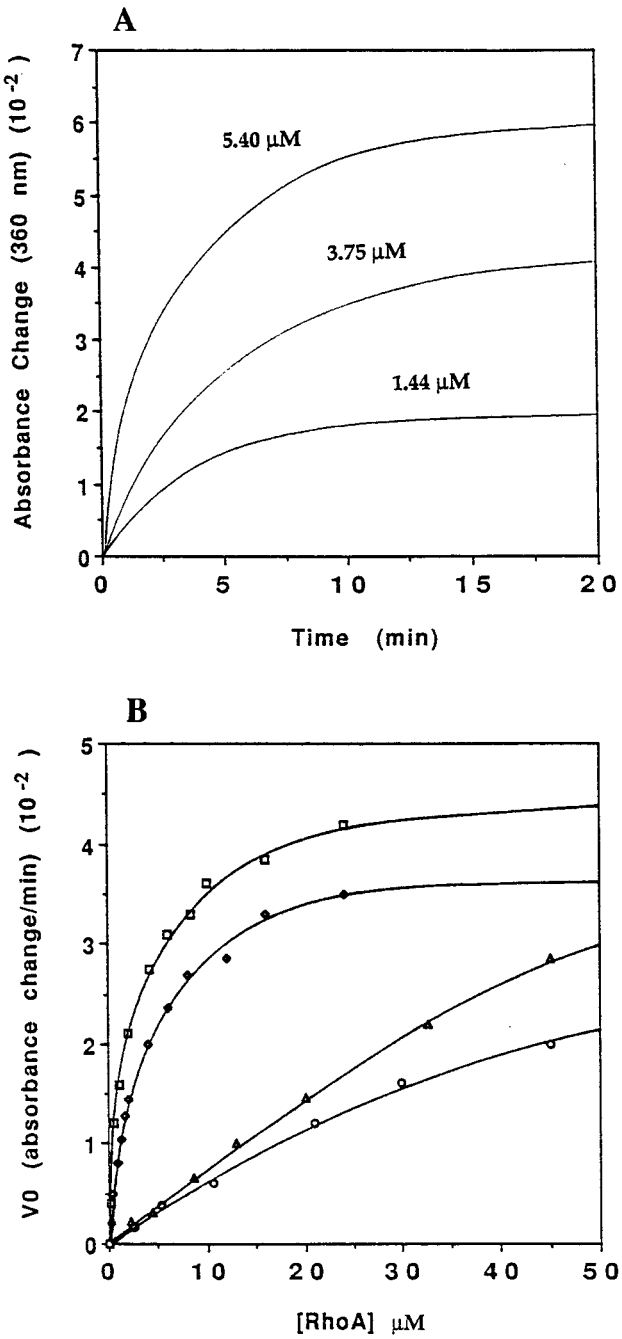

FIGURE 4: Determination of kinetic parameters of GAPs. (A) Absorbance traces of different doses of RhoA in the presence of 30 nM p190GAP at 360 nm wavelength were monitored over time. The reactions were carried out at 20 °C in a buffer containing 50 mM HEPES, pH 7.6, 5 mM $MgCl_2$, 200 μM GTP, 10 units/mL purine nucleoside phosphorylase, and 0.2 mM substrate MESG. (B) Initial rate of GTP hydrolysis by RhoA as a function of RhoA concentration. 35 nM p190GAP (squares), 50 nM p50RhoGAP (diamonds), 62 nM Bcr (triangles), or 287 nM 3BP-1 (circles) was used in the measurements. The GAP-catalyzed GTPase rates were fitted to the modified Michealis-Menten equation (eq 1 described under Experimental Procedures) to yield the K_m and V_{max} values.

rate-limiting step in the GAP-catalyzed reactions. It has to be cautioned that the affinity between RhoA-GMP-PNP and GAPs may be underestimated for the RhoA-GTP and GAP interaction, since GMP-PNP was found to bind to Ras with approximately 10-fold lower affinity relative to GTP; therefore, RhoA-GMP-PNP may not truly represent the GTP-bound state. Nonetheless, there is a correlation between the catalytic efficiency (K_{cat}/K_m) and the binding affinity of the GAPs to RhoA, similar to the case of Cdc42 (*28*), suggesting that tight binding of a GAP domain contributes to the stabilization of a transition state of the small GTPase in facilitating GTP hydrolysis.

The affinity of RhoA-GDP to various GAPs was also determined by a similar assay (Figure 6A). While p190GAP, Bcr, and 3BP-1 bound to RhoA-GDP with a K_d larger than 30 μM, p50RhoGAP was able to bind with relatively high affinity (K_d value of 6 μM) to RhoA-GDP (Table 2). Consistent with what we have observed in the time courses of p50RhoGAP-catalyzed GTP hydrolysis of RhoA (Figure

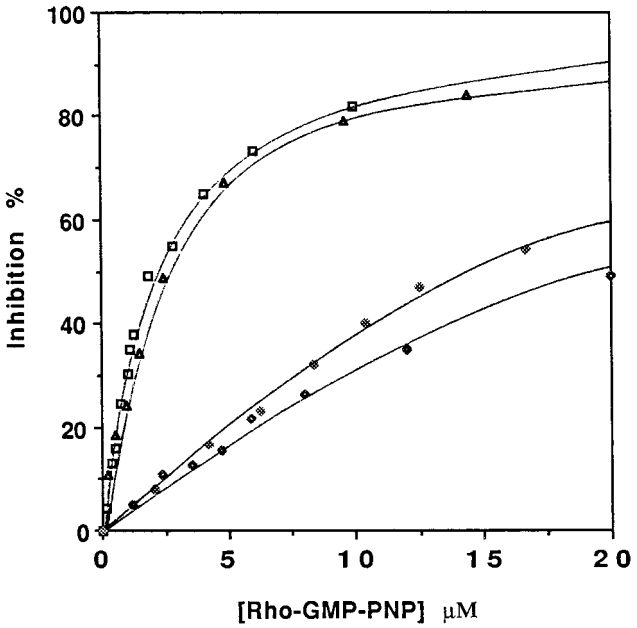

FIGURE 5: Binding of GAPs to the GMP-PNP-bound RhoA measured by inhibition of GAP-stimulated RhoA-[γ-^{32}P]GTP hydrolysis. 20 nM [γ-^{32}P]GTP loaded RhoA together with 50 nM p190GAP (squares), 77 nM p50RhoGAP (triangles), 2.2 μM Bcr (open diamonds), or 4.8 μM 3BP-1 (filled diamonds) was incubated in the assay buffer containing 50 mM HEPES, pH 7.6, 0.2 mg/mL BSA, and 5 mM $MgCl_2$ with increasing concentrations of GMP-PNP-bound RhoA at 20 °C for 5 min before termination of the reaction by filtration through nitrocellulose filters.

Table 2: Affinity of GAPs for RhoA[a]

GAP	K_d (μM)	
	GMP-PNP	GDP
p190	2.18 ± 0.08	33.2 ± 0.5
p50RhoGAP	2.47 ± 0.41	6.15 ± 0.10
p50RhoGAP[b]	3.71 ± 0.35	8.36 ± 0.80
Bcr	21.95 ± 0.51	30.43 ± 0.93
3BP-1	16.3 ± 1.5	66.3 ± 3.8

[a] The dissociation constants (K_ds) were derived by fitting the competitive inhibition data shown in Figures 5 and 6 to eq 2. The competition reactions were performed under conditions as described in Figure 5 except in the case for p50RhoGAP [b]in which an assay buffer containing 50 mM HEPES, pH 7.6, 0.2 mg/mL BSA, 100 mM NaCl, and 5 mM $MgCl_2$ was used. Data are representative of results of two independent experiments.

2B), the effect of product (RhoA-GDP) inhibition for the p50RhoGAP-catalyzed reaction was apparent when different doses of RhoA-GDP at micromolar concentrations were added to the GAP assay mixture containing [γ-^{32}P]GTP-bound RhoA and p50RhoGAP (Figure 6B). Even at a more physiological salt concentration (100 mM NaCl), this effect of product inhibition remains obvious with K_d values of p50RhoGAP to RhoA-GDP at 8.36 μM and to RhoA-GMP-PNP at 3.71 μM (Table 2). This unique property of p50RhoGAP distinguishes itself from the mechanism of p190GAP-stimulated RhoA hydrolysis.

Salt Dependence of p190GAP- and p50RhoGAP-Catalyzed GTP Hydrolysis of RhoA. The interaction of GAPs with RhoA may involve specific pairs of charged residues such as the case for the Ras GTPase and RasGAP interaction (*32*). To further distinguish the mechanisms employed by p190GAP and p50RhoGAP in RhoA catalysis, we measured the kinetic parameters of the respective GAP reactions under various

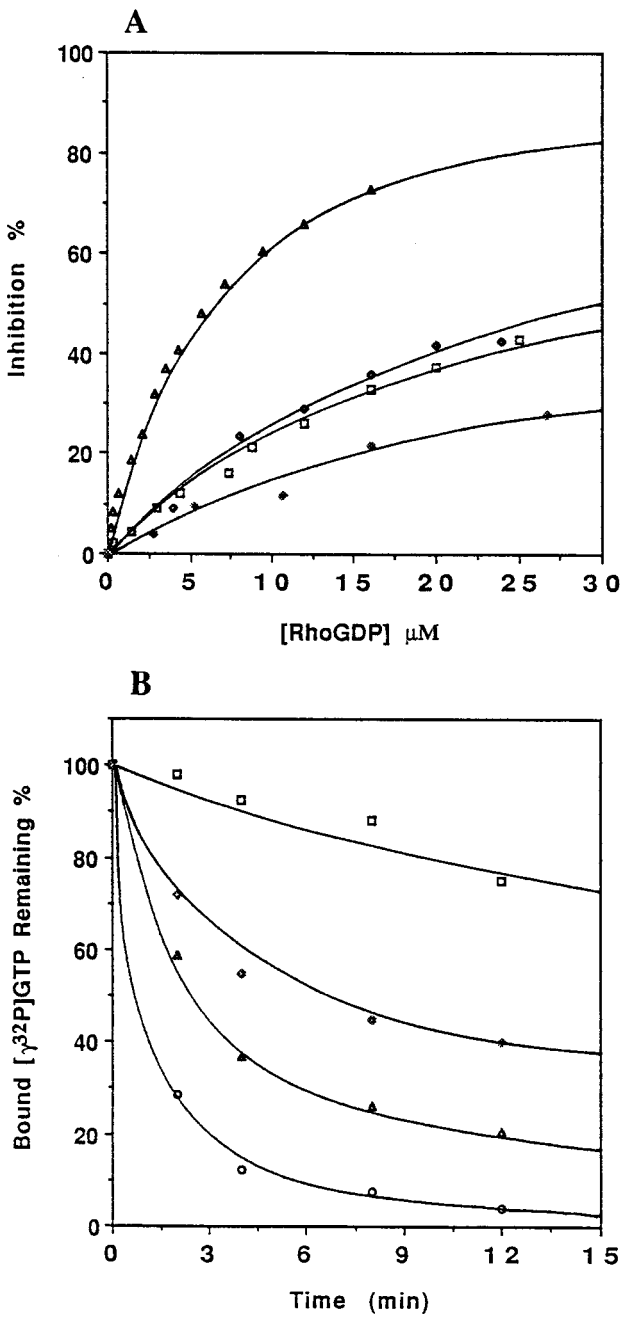

FIGURE 6: Inhibition of the p50RhoGAP-stimulated GTPase activity of RhoA by RhoA-GDP. (A) Determination of the binding affinity of GAPs to RhoA-GDP. 20 nM [γ-^{32}P]GTP-bound RhoA was incubated with 60 nM p190GAP (squares), 100 nM p50RhoGAP (triangles), 1.6 μM Bcr (open diamonds), or 7.1 μM 3BP-1 (filled diamonds) with increasing concentrations of RhoA-GDP at 20 °C for 5 min. Reaction conditions were similar to those in Figure 5. (B) Time courses of intrinsic (squares) and p50RhoGAP-catalyzed [γ-^{32}P]GTP hydrolysis by RhoA in the presence of 0 μM (circles), 4 μM (triangles), or 8 μM (diamonds) RhoA-GDP. 100 nM [γ-^{32}P]-GTP-loaded RhoA was incubated in a HEPES buffer (pH 7.6) with 20 nM p50RhoGAP and various amounts of RhoA-GDP.

NaCl and Mg^{2+} concentrations as examplified in Figure 7. While the K_{cat} of the p190GAP-catalyzed reaction of RhoA was not affected significantly by the increase of either NaCl concentration (from 0 to 300 mM) or $MgCl_2$ concentration (from 1 to 10 mM), the K_m values increased over 30-fold when the NaCl concentration was raised from 0 to 300 mM (Table 3). In contrast, the same changes in reaction conditions resulted in a less than 5-fold increase in the K_m

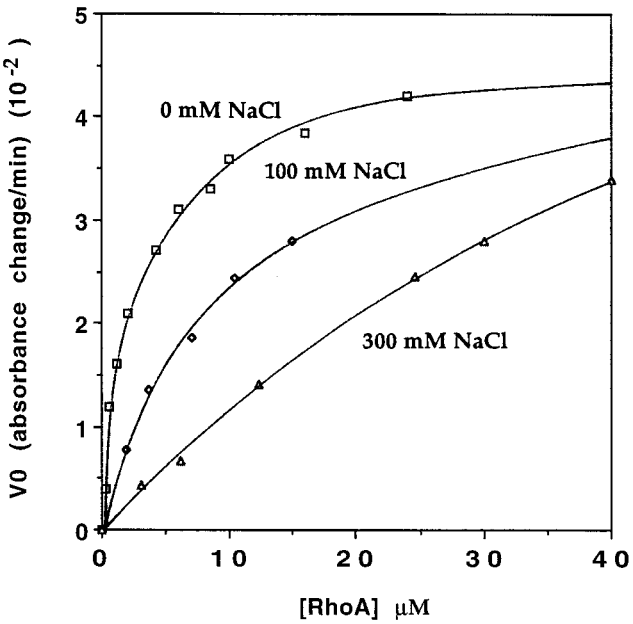

FIGURE 7: Effect of NaCl concentration on the kinetics of RhoA-GTP hydrolysis stimulated by p190GAP. The initial rate (V_0) of P_i release by RhoA-GTP was determined at increasing concentrations of RhoA in a HEPES buffer (pH 7.6) containing 5 mM $MgCl_2$ supplemented with NaCl at the indicated concentrations and 35 nM p190GAP. Data were fitted to eq 1 to derived the Michaelis−Menten parameters.

of the p50RhoGAP-catalyzed reaction with K_{cat} essentially unchanged (Table 3). Thus, the p190GAP−RhoA interaction seems to be much more sensitive to changes in salt concentration which primarily affects the reaction K_m and probably the binding affinity of the interaction, suggesting that one or more pairs of charged residues between RhoA and p190GAP may be involved in specifying the reaction.

Sensitivity of RhoA Effector Domain Mutants to p190GAP and p50RhoGAP. Given the differences of p190GAP and p50RhoGAP in reaction with RhoA, i.e., the unique product inhibition property by p50RhoGAP and extra sensitivity to NaCl and Mg^{2+} by p190GAP, we looked for differences in the structural elements of RhoA involved in interaction with the respective GAPs which may contribute to the kinetic distinctions. Among the four effector domain mutants of RhoA examined (Figure 8), Y34K, T37A, and F39E suffered partial loss of responsiveness to p50RhoGAP while Y42K remained similar to wild-type RhoA, suggesting that this region of RhoA is required for interaction with p50RhoGAP and that the residues Y34, T37, and F39 are involved in effective coupling with p50RhoGAP. This is somewhat different from what we have found in an earlier study for the interaction of RhoA with p190GAP, in which the Y34K and T37A mutants of RhoA were shown to be completely insensitive to p190GAP stimulation (*33*). Therefore, there appears to exist a structural basis for differences in kinetic behaviors of the p190GAP−RhoA and the p50RhoGAP−RhoA interactions.

DISCUSSION

The biochemical mechanism of Rho functions has been under intensive study with increasing evidence pointing to a highly regulated cycle of RhoA between the active GTP-bound state and the inactive GDP-bound state: a family of guanine nucleotide exchange factors represented by the Dbl oncoprotein has been shown to catalyze the GDP/GTP exchange activity and thus activate RhoA (*10*), and the transition from the GTP-bound form to the GDP-bound form of Rho appears to be regulated by the RhoGAPs which directly stimulate the intrinsic GTPase activity of RhoA (*16*). In addition to the GAPs characterized here, recently indentified RhoGAPs include the 85 kDa regulatory subunit of PI 3-kinase (*34*, *35*), the human brain-specific protein n-chimaerin (*36*), the 95 kDa potential downstream target of the Ras-related Ral GTPase (*37*), the PLC-δ activator p122 (*38*), the unconventional myosin myr 5 (*39*), the SH3 domain-containing focal adhesion kinase partner Graf (*40*), and the *BEM2* and *BEM3* gene products of yeast bud-site assembly (*41*, *42*). Each of these GAPs may have a role in Rho family GTPase-mediated signaling pathways. Although the nature of the enzymatic activity of GAPs suggests that they may act as negative regulators of Rho GTPases, there is also evidence that some of them may function as effector targets (*34*, *35*, *43*). In the present study, we have attempted to quatify some of the RhoA−GAP interactions in order to provide insights into the catalytic and binding properties of individual GAPs by directly comparing the kinetic parameters of the interactions and looking for unique features of the functional coupling involved, and, thus, to help clarify the role of individual GAPs in RhoA signaling pathways.

Of the four mammalian RhoGAPs examined here (p190GAP, p50RhoGAP, Bcr, and 3BP-1), we found that while both p190GAP and p50RhoGAP represent excellent catalytic activity toward RhoA, p190GAP contains ~3-fold higher catalytic efficiency (K_{cat}/K_m), which is consistent with previous observations (*21*). However, Bcr and 3BP-1, contrary to earlier reports that they might not be able to catalyze RhoA GTPase activity (*21*, *25*), are also found to contain GAP activity for RhoA, although they are at least 1 order of magnitude weaker than p190GAP or p50RhoGAP. The apparent discrepancy may be due to the difference in assay conditions employed, as in the previously reported cases only low concentrations of RhoA and a substoichiometric amount of Bcr or 3BP-1 were used, which may not result in significant binding and catalytic activities toward RhoA. The supreme catalytic efficiencies of p190GAP and p50RhoGAP appear to reside in their lower K_m values (1.79 and 2.83 μM, respectively, compared with 89 μM for Bcr and 3BP-1), and these K_m values show excellent agreement with the K_d values of binding to RhoA-GMP-PNP. Reminiscent of the Cdc42−GAP interactions in this respect (*28*), the RhoA−p190GAP and RhoA−p50RhoGAP interactions suggest a mechanism of GAP-catalyzed GTP hydrolysis which involves fast equilibrium binding to Rho GTPases followed by a rate-limiting step of γ-P_i cleavage of bound GTP. This is similar to the well-characterized Ras−RasGAP interaction in which it has been shown that a fast equilibrium between Ras and RasGAP precedes the GAP-catalyzed bond cleavage reaction (*44*). In the case of Ras-catalyzed GTP hydrolysis, RasGAP appears to play a direct role by forming a ternary complex and supplying residues for GTP hydrolysis on Ras and thereby stabilizing the transition state of the reaction (*32*, *45*). In particular, a highly conserved Arg residue of RasGAP, Arg789, which has been shown to be critical for GAP activity and was found to point to the active site of Ras in the tertiary structure, has been demonstrated

Table 3: Effects of Salt and Mg^{2+} Concentrations on GAP-Regulated Kinetics of RhoA GTPase[a]

		p190GAP		p50RhoGAP	
[NaCl] (mM)	[$MgCl_2$] (mM)	K_{cat} (min^{-1})	K_m (μM)	K_{cat} (min^{-1})	K_m (μM)
0	5	96.6 ± 1.8[b]	1.79 ± 0.14[b]	59.6 ± 1.2[b]	2.83 ± 0.16[b]
100	1	51.2 ± 1.5	3.48 ± 0.22	27.2 ± 0.5	4.40 ± 0.07 100
100	5	52.5 ± 3.2	7.38 ± 0.97	28.8 ± 1.5	4.81 ± 0.22
100	10	82.0 ± 12.6	28.5 ± 4.5	24.8 ± 1.0	10.4 ± 0.7
300	5	82.7 ± 8.1	51.7 ± 7.9	17.0 ± 1.2	13.8 ± 1.7

[a] GAP reactions and data treatments were carried out as in Table 1 except for variations in NaCl and $MgCl_2$ concentrations. [b] Data are as listed in Table 1.

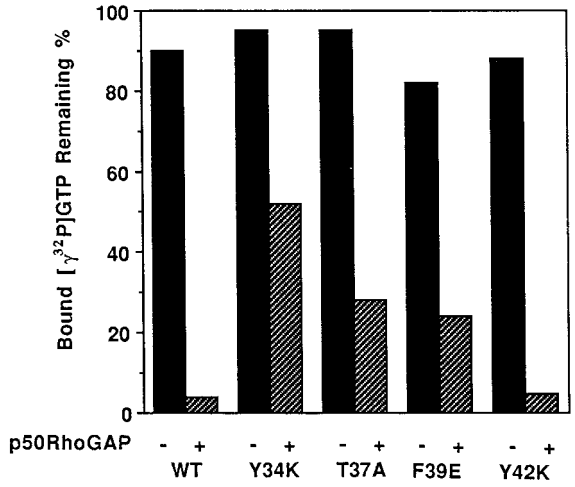

FIGURE 8: GAP-responsiveness of the effector domain mutants of RhoA toward p50RhoGAP. 1.0 μM wild-type (WT) RhoA or effector domain mutants were preloaded with [γ-^{32}P]GTP and were then incubated in the presence or absence of 50 nM p50RhoGAP in a HEPES buffer (pH 7.6) with 100 mM NaCl and 5 mM $MgCl_2$ for 5 min before the termination of reactions by nitrocellulose filtration.

to participate in Ras catalysis by forming an arginine-finger loop to bond with Gln61 of Ras, AlF_4^-, and β-phosphate of GDP in the Ras-GDP, AlF_4^-, and RasGAP complex (*32*). The role of RhoGAPs in RhoA GTP hydrolysis appears similar in this regard given that a stable crystal complex between RhoA-GDP, AlF_4^-, and p50RhoGAP has been obtained recently (*46*) which may mimic the transition state of the RhoA GTPase reaction, and that the highly conserved Arg85 residue of the GAP domains of both p190 and p50RhoGAP was found to be essential for catalysis while dispensable for binding probably through stabilization of a transition state of RhoA by interaction with the main chain carbonyl of Arg85 of GAP (*33*). Additional residues of p50RhoGAP found to be involved in interaction with RhoA in the crystal structure of the complex (*46*) include the conserved Asn194 and Lys122 which may serve to provide structural elements of RhoGAPs to functionally interact with RhoA, as appears to be the case for p190GAP (*33*).

In addition to these general features, we also observed some unique properties of RhoA GTPase catalysis by p190GAP and by p50RhoGAP: p50RhoGAP displays comparable binding affinities to RhoA-GTP and to RhoA-GDP (*23*), resulting in the kinetic property of product inhibition, and the p190GAP−RhoA interaction is much more sensitive to the salt and Mg^{2+} environment due to perturbation of the K_m and probably the K_d of the interaction. These differences in kinetic properties suggest that different structural elements of RhoA are involved in interaction with the respective GAPs. Indeed, we found that mutations of certain amino acid residues of the effector domain region of RhoA, i.e., Y34K and T37A, demonstrated a discerning effect on p190GAP and p50RhoGAP (partially responsive to one while completely unresponsive to another). In another study mapping the sites of interaction between RhoA and p190GAP (*33*), we have identified the unique residue Asp90 of RhoA as an important determinant for specifying RhoA−p190GAP interaction. Consistent with the sensitivity of p190 catalysis of RhoA to NaCl and Mg^{2+} observed here, it is likely that the charged residue Asp90 of RhoA may form a specific salt bridge with a basic residue on the surface of p190GAP to make a major contribution to the relative tight binding of RhoA to p190GAP and to facilitate the catalysis by p190GAP.

The *in vivo* functions of RhoGAPs are not clear. Microinjection experiments performed using RhoGAP domains suggest that while p190GAP and p50RhoGAP seem to be able to inhibit RhoA-regulated actin-stress fiber formation in fibroblast cells, both Bcr and 3BP-1 can downregulate Rac1-mediated membrane ruffling (21, 25). Our observations that the GAP domains of Bcr and 3BP-1 contain weak GAP activity toward RhoA with a K_m of 89 μM but have supreme catalytic efficiencies toward Rac1 (*47*) are consistent with the possibility that the Bcr and 3BP-1 GAP domains are specific Rac downregulators. The 2−3 μM binding affinity and high catalytic efficiency of p190GAP and p50RhoGAP for RhoA are also consistent with a role of these GAPs in downregulating RhoA function. Moreover, given the even higher catalytic efficiency (K_{cat}/K_m of $\sim$700 min^{-1} μM^{-1}) of p50RhoGAP toward Cdc42 (*28*), it is also likely that p50RhoGAP may have dual roles in the regulation of both RhoA and Cdc42 GTPases.

Whether the observed effect of product (RhoA-GDP) inhibition of p50RhoGAP catalysis is relevant in *in vivo* situations is not clear at present. It is expected that a potential effector target of RhoA should have a much higher affinity toward the GTP-bound state than the GDP-bound state if the case of Ras interaction with effectors can be viewed as an analogy. In this regard, therefore, p50RhoGAP may not function as an effector candidate for RhoA signaling. On the other hand, it remains a possibility that the relatively tight and selective binding of p190GAP to RhoA-GTP constitutes it as a candidate for transducing signals from the activated RhoA during the course of coupling. It will be of particular interests to examine this possibility using the full-length form of the GAP in a cellular context since a RhoGAP family member, n-chimearin, has recently been shown to act synergistically with Rac1 to induce lamellipodia formation in fibroblast cells (*43*). In addition, the specificity and GAP

catalytic activity of full-length GAPs also warrant further investigation due to the multifunctional domain feature of the RhoGAPs which may involve both inter- and intramolecular regulations of the GAP domains.

In summary, the data presented here provide direct comparison of the binding and catalytic activities of a panel of mammalian RhoGAP domains to RhoA. The results suggest that there exists a unique mechanism of functional interaction between RhoA and individual RhoGAP which may involve distinct structural determinants of the small G-protein to cause the apparent differences in kinetic properties.

REFERENCES

1. Ridley, A. J. (1996) *Curr. Biol. 6*, 1256−1264.
2. Symons, M. (1996) *Trends Biochem. Sci. 21*, 178−181.
3. Tapon, N., and Hall, A. (1997) *Curr. Opin. Cell Biol. 9*, 86−92.
4. Morii, N., Teru-uchi, T., Tominaga, T., Kumagai, N., Kozaki, S., Ushikubi, F., and Narumiya, S. (1992) *J. Biol. Chem. 267*, 20921−20926.
5. Tominaga, T., Sugie, K., Hirata, M., Morii, N., Fukata, J., Uchida, A., Imura, H., and Marumiya, S. (1993) *J. Cell Biol. 120*, 1529−1537.
6. Takaishi, K., Kikuchi, A., Kuroda, S., Kotani, K., Sasaki, T., and Takai, Y. (1993) *Mol. Cell. Biol. 13*, 72−79.
7. Santos, M. F., McCormack, S. A., Guo, Z., Okolicany, J., Zheng, Y., Johnson, L. R., and Tigyi, G. (1997) *J. Clin. Invest. 100*, 216−225.
8. Kishi, K., Sasaki, T., Kuroda, S., Itoh, T., and Takai, Y. (1993) *J. Cell Biol. 120*, 1187−1195.
9. Ridley, A. J., and Hall, A. (1992) *Cell 70*, 389−399.
10. Cerione, R. A., and Zheng, Y. (1996) *Curr. Opin. Cell Biol. 8*, 216−222.
11. Qiu, R., Chen, J., McCormick, F., and Symons, M. (1995) *Proc. Natl. Acad. Sci. U.S.A. 92*, 11781−11785.
12. Khosravi-Far, R., Solski, P. A., Clark, G. J., Kinch, M. S., and Der, C. J. (1995) *Mol. Cell. Biol. 15*, 6443−6453.
13. Hill, C. S., Wynne, J., and Treisman, R. (1995) *Cell 81*, 1159−1170.
14. Olson, M. F., Ashworth, A., and Hall, A. (1995) *Science 269*, 1270−1272.
15. Boguski, M. S., and McCormick, F. (1993) *Nature 366*, 643−654.
16. Lamarche, N., and Hall, A. (1994) *Trends Genet. 10*, 436−440.
17. Zheng, Y., Hart, M. J., Shinjo, K., Evans, T., Bender, A., and Cerione, R. A. (1993) *J. Biol. Chem. 268*, 24629−24634.
18. Musacchio, A., Cantley, L. C., and Harrison, S. C. (1996) *Proc. Natl. Acad. Sci. U.S.A. 93*, 14373−14378.
19. Barrett, T., Xiao, B., Dodson, E. J., Dodson, G., Ludbrook, S. B., Nurmahomed, K., Gamblin, S. J., Musacchio, A., Smerdon, S. J., and Eccleston, J. F. (1997) *Nature 385*, 458−461.
20. Settleman, J., Albright, C. F., Foster, L. C., and Weinberg, R. A. (1992) *Nature 369*, 153−154.
21. Ridley, A. J., Self, A. J., Kasmi, F., Paterson, H. F., Hall, A., Marshall, C. J., and Ellis, C. (1993) *EMBO J. 12*, 5151−5160.
22. Barfod, E. T., Zheng, Y., Kuang, W.-J., Hart, M. J., Evans, T., Cerione, R. A., and Ashkenazi, A. (1993) *J. Biol. Chem. 268*, 26059−26062.
23. Lancaster, C. A., Taylor-Harris, P. M., Self, A. J., Brill, S., van Erp, H. E., and Hall, A. (1994) *J. Biol. Chem. 269*, 1137−1142.
24. Diekmann, D., Brill, S., Garrett, M. D., Totty, N., Hsuan, J., Monfries, C., Hall, C., Lim, L., and Hall, A. (1991) *Nature 351*, 400−402.
25. Cicchetti, P., Ridley, A., Zheng, Y., Cerione, R. A., and Baltimore, D. (1995) *EMBO J. 14*, 3127−3135.
26. Webb, M. R. (1992) *Proc. Natl. Acad. Sci. U.S.A. 89*, 4884−4887.
27. Li, R., and Zheng, Y. (1997) *J. Biol. Chem. 272*, 4671−4679.
28. Zhang, B., Wang, Z.-X., and Zheng, Y. (1997) *J. Biol. Chem. 272*, 21999−22007.
29. Zheng, Y., Bender, A., and Cerione, R. A. (1995) *J. Biol. Chem. 270*, 626−630.
30. Webb, M. R., and Hunter, J. (1992) *Biochem. J. 287*, 555−559.
31. Chuang, T.-H., Xu, X., Kaartinen, V., Heisterkamp, N., Groffen, J., and Bokoch, G. M. (1995) *Proc. Natl. Acad. Sci. U.S.A. 92*, 10282−10286.
32. Scheffzek, K., Ahmadian, M. R., Kabsch, W., Wiesmuller, L., Lautwein, A., Schmitz, F., and Wittinghofer, A. (1997) *Science 277*, 333−338.
33. Li, R., Zhang, B., and Zheng, Y. (1997) *J. Biol. Chem. 272*, 32830−32835.
34. Zheng, Y., Bagrodia, S., and Cerione, R. A. (1994) *J. Biol. Chem. 269*, 18727−18730.
35. Tolias, K. F., Cantley, L. C., and Carpenter, C. L. (1995) *J. Biol. Chem. 270*, 17656−17659.
36. Leung, T., How, B.-E., Manser, E., and Lim, L. (1993) *J. Biol. Chem. 268*, 3813−3816.
37. Cantor, S. B., Urano, T., and Feig, L. A. (1995) *Mol. Cell. Biol. 15*, 4578−4584.
38. Homma, Y., and Emori, Y. (1995) *EMBO J. 14*, 286−291.
39. Reinhard, J., Scheel, A. A., Diekmann, D., Hall, A., Ruppert, C., and Bahler, M. (1995) *EMBO J. 14*, 697−704.
40. Hildebrand, J. D., Taylor, J. M., and Parsons, J. T. (1996) *Mol. Cell. Biol. 16*, 3169−3178.
41. Zheng, Y., Cerione, R. A., and Bender, A. (1994) *J. Biol. Chem. 269*, 2369−2372.
42. Peterson, J., Zheng, Y., Bender, L., Myers, A., Cerione, R., and Bender, A. (1994) *J. Cell Biol. 127*, 1395−1406.
43. Kozma, R., Ahmed, S., Best, A., and Lim, L. (1996) *Mol. Cell. Biol. 16*, 5069−5080.
44. Ahmadian, M. R., Hoffmann, U., Goody, R. S., and Wittinghofer, A. (1997) *Biochemistry 36*, 4535−4541.
45. Mittal, R., Ahmadian, M. R., Goody, R. S., and Wittinghofer, A. (1996) *Science 273*, 115−117.
46. Rittinger, K., Walker, P. A., Eccleston, J. F., Smerdon, S. J., and Gamblin, S. J. (1997) *Nature 389*, 758−762.
47. Zhang, B., Chernoff, J., and Zheng, Y. (1998) *J. Biol. Chem.* (in press).

BI9718447